

The DIGISOIL project (FP7-ENV-2007-1 N°211523) is financed by the European Commission under the 7th Framework Programme for Research and Technological Development, Area "Environment", Activity 6.3 "Environmental Technologies".



Description of processing protocols for each sensor

FP7 – DIGISOIL Project Deliverable 1.2

NFP7-DIGISOIL-D1.2

May 2009

G.Grandjean (BRGM)

With the collaboration of

A.Bitri (BRGM), I.Cousin (INRA), S.Lambot, F.André (UCL)

Checked by:

Name: S.Lambot

Date: 20/05/09



Approved by:

Name: G.Grandjean

Date: 25/05/09



BRGM's quality management system is certified ISO 9001:2000 by AFAQ.



The DIGISOIL project (FP7-ENV-2007-1 N211523) is financed by the European Commission under the 7th Framework Programme for Research and Technological Development, Area "Environment", Activity 6.3 "Environmental Technologies".



Keywords:

In bibliography, this report should be cited as follows:

Grandjean, G., Bitri, A., Cousin, I., Lambot, S., André, F., 2009. Description of processing protocols for each sensor. Report N°FP7-DIGISOIL-D1 .2, 40 pages.

© BRGM, 2009. No part of this document may be reproduced without the prior permission of BRGM.

Synopsis

The present deliverable concerns the last task of the DIGISOIL's WP1. Possible and adapted processing or inversion techniques for geophysical data are studied.

A state of the art on general theory related to inverse problem is first given. Then, for the 4 methods developed in DIGISOIL (GPR, EMI, Geoelectric and seismic), the problem is deeply described and solutions are proposed.

Some examples of inverted data are shown to illustrate these solutions.

Contents

1. Introduction	9
1.1. MAIN OBJECTIVES OF THIS STUDY	9
1.2. MANAGING MEASUREMENTS AND PROCESSING PROTOCOLS.....	9
2. Review of inverse methods in geophysics	11
2.1. LINEAR AND NON LINEAR INVERSE PROBLEM	11
2.1.1. General overview	11
2.1.2. Fundamentals of linearized inverse methods.....	12
2.2. OPTIMIZATION METHODS	15
2.2.1. Monte-Carlo (MC) and simulated annealing (SA) approaches.....	15
2.2.2. Neural network	16
2.2.3. Genetic algorithms (GA)	16
2.2.4. Multilevel Coordinate Search (MCS)	16
2.3. REVIEW OF CLASSICAL – COMMERCIAL OR NON-COMMERCIAL – CODES FOR GEOPHYSICAL DATA INVERSION	16
2.3.1. Geoelectric.....	16
2.3.2. GPR	17
2.3.3. EMI	18
2.3.4. Seismic	18
3. Adapted methodologies for DIGISOIL	19

3.1. ELECTRICAL METHODS.....	19
3.2. GPR – EMI	20
3.2.1. Electromagnetic GPR and EMI forward modeling : a united method.....	20
3.2.2. Model inversion	23
3.3. SEISMIC METHODS.....	24
3.3.1. Pre-processing operations.....	24
3.3.2. Strategy for inversion.....	25
3.3.3. Proposed solution: methodology and code	27
4. Conclusions	31
5. References	33

List of illustrations

Figure 1 : Three-dimensional N-layered medium with a point source and receiver S. Each layer is characterized by the dielectric permittivity ϵ , electrical conductivity σ , and thickness h	21
Figure 2. Measured and modelled GPR Green's functions for wave propagation in a two-layered sand. (a) Frequency domain. (b) Time domain. (Lambot et al., 2004).	22
Figure 3. Measured (blue curves) and modelled (red curves) EMI Green's functions for measurements at different heights above a copper sheet. (Moghadas et al., 2009).	23
Figure 4. (a) Off-ground GPR system used for real-time mapping of the soil properties. (b) GPR-derived map of soil surface water content over a field of about 16ha, including more than 3000 measurements.....	24
Figure 5 : Subsurface model commonly used for surface wave inversion	25
Figure 6 : From acquisition to inversion of surface wave.	28
Figure 7 : Automatic extraction of dispersion curves and shape processing.	29
Figure 8 : Spatial covering of a studied area (left) and associated soil property map (right).....	29

1. Introduction

1.1. MAIN OBJECTIVES OF THIS STUDY

This deliverable presents some elements for retrieving geophysical parameters from sensors measurements.

In order to reach the physical frontiers of information retrieval from the different sensors, signal processing, when possible, is based on advanced mechanistic inverse modelling techniques. Efforts are therefore focus on improved signal understanding, forward modelling, and inversion using global optimization and regularization to estimate the soil geophysical parameters.

Joint interpretation strategies, i.e., how to combine several inverted geophysical parameters into a more robust interpretation in terms of soil characteristics, will be further developed in WP2 dealing with data fusion.

In the following sections we first present the different kinds of inversion strategies before to get more in details with applications to typical geophysical methods.

1.2. MANAGING MEASUREMENTS AND PROCESSING PROTOCOLS

The principle of inversion processes consists in simulating data from a mathematical model that uses *a priori* parameters with their associated uncertainties. These calculated data are then compared to measured ones by using a L_2 norm. From this comparison, the cost – or likelihood – function. The problem consist in reducing the cost function by adjusting the parameters. For this purpose, several methods can be used: gradient method, optimisation methods, etc.

As it will be mentioned in next sections, inverting correctly geophysical data require additional considerations for ensuring that the resulting models are constrained enough:

- An efficient inverse algorithm may need to be applied on pre-processed data in order to make the observed data in good agreement with the mathematical model hypothesis;
- If possible, uncertainties on observations need to be integrated in the process; these *a priori* information is an important input since it offers to algorithms a larger level of freedom for fitting observed and calculated data;
- The *a priori* parameters set needs to be as close as possible to the real one, meaning that additional information coming from existing data have to be initially integrated to constrain parameters;

- The number of data used in the process have to be in proportion to the number of parameters to invert, otherwise the problem is underestimated and the risk of divergence increases;
- The resulting parameters have to be considered with their *a posteriori* uncertainties for identifying unconstrained ones.

In the next section, fundamentals of inverse problems are presented in a generic way. The last section is dedicated to describe inverse techniques that will be implemented in DIGISOIL for typical methods (seismics, GPR, geoelectric for example). For other methods, no inversion process is foreseen since measurements will be integrated directly in the fusion process leading to interpreted maps.

2. Review of inverse methods in geophysics

2.1. LINEAR AND NON LINEAR INVERSE PROBLEM

2.1.1. General overview

The inversion of geophysical data is concerned with the problem of making inferences about physical systems from observed data. Since nearly all data are subject to some uncertainty, these inferences are usually statistical (Scales and Smith, 1996.). Further, since one can only record finitely many data and since physical systems are usually modelled by continuum equations no geophysical inverse problems are really uniquely solvable: if there is a single model that fits the data there will be infinity of them. Our goal is then to characterize the set of models that fit the data and satisfy our prejudices as well as other information.

To make these inferences quantitative one must answer three fundamental questions. How accurately are the data known? I.e., what does it mean to "fit" the data. How accurately can we model the response of the system? In other words, have we included all the physics in the model that contribute significantly to the data? Finally, what is known about the system independent of the data? This is called a priori information and is essential since for any sufficiently fine parameterization of a system there will be unreasonable models that fit the data too.

Inverse theory is an exceedingly large topic and we cannot cover all aspects in depth. General references for geophysical inversion theory included the textbooks by Tarantola (1987), Menke(1989) or Scales and Smith (1996). In general, the inversion implies the minimization of an objective function representing the discrepancies between the data and the model. With such a strategy, both data and process knowledge information are inherently merged in a mechanistic way.

The three conditions to ensure a proper estimation of the quantities of interest, according to Hadamard, are : existence, uniqueness and stability of the inverse solution. Provided that the model parameters are identifiable and enough information is contained in the data, which includes enough model sensitivity to the data, these three conditions are satisfied and the inverse problem is said to be well-posed. Yet, it is also essential that the model describes sufficiently well the physical process, and, furthermore, the minimization algorithm should be able to find the solution in a reasonable time. Uncertainties in the estimated parameters can be derived from the objective function topography.

The mathematical model may simultaneously describe several types of data and several models may be integrated in such an inverse modelling framework. For instance, Lambot et al. (2006) constrained the inversion of an electromagnetic GPR model with a soil hydrodynamic model to simultaneously reconstruct vertical water

content profiles and identify the unsaturated soil hydraulic properties from time-lapse, off-ground GPR data.

Integrated inverse modelling is part of the DIGISOIL strategy to infer the soil properties from the different sensors and the knowledge of the underlying geophysical and soil/hydrodynamic processes. A part of the information fusion process situates in the formulation of the objective function, for which several methods are available (Bayesian, Pareto, etc.).

2.1.2. Fundamentals of linearized inverse methods

A geophysical experiment consists of an energy source, an earth model, and a response from the ground. The energy source can be natural as in the case for magnetic, or can be a man made device, such as a vibrator or weight drop used in seismic survey, or an electric current used in electrical studies. The earth model is characterized by 3D distribution of physical properties and the responses can be physical fields that are measured on surface or in boreholes. The propagation energy through the earth depends upon the 3D distribution of one or more physical properties, i.e. each datum is sensitive to a property variation in the volume. Because each datum is sensitive to what is happening in the volume, it should not be expected that a data image can directly provide localized information about the subsurface geology. Geophysical inversion is required to extract that information from the data.

Data from a geophysical experiment can be generically written in the form (Oldenburg and Li, 2005):

$$F_j[m] = d_j^{obs} \equiv d_j + n_j, j=1,2,\dots,N \quad \text{Eq. 1}$$

where F_j is a forward modelling operator, m is the generic symbol for a physical propriety distribution and the right end side represents the observed datum which consist of the true datum d_j plus additive noise n_j . The forward problem involves calculating the responses under the assumption that the source and the earth model are known.

In a geophysical experiment we acquire N data (d^{obs}), and some knowledge about their uncertainties. The inverse problem attempts to find the model m that produced the noisy observations. This process is much more difficult that forward modelling. Each geophysical datum depends upon a volumetric distribution of the physical property and information about the property is encoded in the data in a complex way. It is unrealistic to expect that we can determine a 3D physical property distribution uniquely when we have only a few data: the inverse problem is considered as ill-conditioned or unstable. If we can find one solution that "acceptably" fits the data, there are infinitely many others that will fit just as well. Selection of a single will required additional information.

This is, arbitrarily small errors in the data can generate arbitrary large errors in the recovered model. The ambiguity could be reduced either by imposing constraints,

finding good initial models (Xia et al., 1999), or including an extra independent data set in inversion procedure (Lai et al., 2005, Del Moro and Pipan 2007).

Data from most geophysical methods are intrinsically nonlinear functional of the physical properties. The issues for solving the nonlinear inverse problem are fundamentally the same as those in the linear problem. We specify a misfit function Φ_d and a model norm Φ_m and we will minimize:

$$\Phi(m) = \Phi_d - \beta \Phi_m \quad \text{Eq. 2}$$

where β is a constant and is generally known as the regularization parameter. The misfit function Φ_d is:

$$\phi_d = \sum_{j=1}^N \left(\frac{d_j^{obs} - F_j[m]}{\epsilon_j} \right)^2 = \|W_d (d^{obs} - F[m])\|^2 \quad (3) \quad \text{Eq. 3}$$

where $W_d = \text{diag}(1/\epsilon)$ and ϵ_j is standard deviation errors of the j 'th datum.

We are able to minimize equation (Eq.2) in one step only if $\Phi(m)$ is a quadratic function. The optimisation problem becomes nonlinear when either Φ_m or Φ_d is nonquadratic. That can occur because the forward mapping for the data is nonlinear or because the model objective function is nonquadratic. A nonlinear problem "became linear" by fixing β so that the objective functions is quadratic (Oldenburg and Li, 2005). This leads to a system of equation that is repeatedly solved with different β s, and in finally an acceptable β is selected.

Hereafter, we shall outline some general principles of Gauss-Newton procedure that are widely used in geophysical methods (Oldenburg and Li 2005).

Let

$$\phi(m) = \phi_d + \beta \phi_m(m) = \|W_d (d^{obs} - F[m])\|^2 + \beta \|W_m (m - m_{ref})\|^2 \quad \text{Eq. 4}$$

with β fixed. Our goal is to find m that minimizes this functional. With nonlinear dependences, the minimization must proceed iteratively so we let $m^{(n)}$ be the current model and δm be a perturbation. Expanding equation (Eq.4) in a Taylor series yields

$$\phi(m^n + \delta m) = \phi(m^{(n)}) + g^T \delta m + \frac{1}{2} \delta m^T H \delta m + \dots \quad \text{Eq. 5}$$

Where $g = \Delta \Phi(m)$ is the gradient and $H = \Delta \Delta \Phi(m)$ with components

$$H_{ij} = \frac{\partial^2 \phi(m)}{\partial m_i \partial m_j} \quad g_j = \frac{\partial \phi(m)}{\partial m_i} \quad \text{Eq. 6}$$

These values are evaluated at the current model $\mathbf{m}^{(n)}$. We want to find a perturbation such that equation (Eq.5) is minimized. Neglecting the higher order terms and taking the derivative of equation (Eq.5) with respect $\delta \mathbf{m}$, and set the resultant to zero, yields the Newton's equation for the perturbation:

$$H \delta \mathbf{m} = -\mathbf{g} \quad \text{Eq. 7}$$

The solution is updated by setting $\mathbf{m}^{(n+1)} = \mathbf{m}^{(n)} + \delta \mathbf{m}$ and the process is continued until convergence (gradient close to zero).

To evaluate the Newton equation (Eq.7) we need to compute the gradient and Hessian. The gradient of equation (Eq.4) is:

$$\mathbf{g}(m) = \mathbf{J}^T \mathbf{W}_d^T \mathbf{W}_d (\mathbf{F}[m] - d^{obs}) + \beta \mathbf{W}_m^T \mathbf{W}_m (m - m_{ref}) \quad \text{Eq. 8}$$

Where $\mathbf{J}(\mathbf{m}) = \partial \mathbf{F} / \partial \mathbf{m}$ is the sensitivity matrix.

The Hessian has the form:

$$\mathbf{H} = \mathbf{J}^T \mathbf{W}_d^T \mathbf{W}_d \mathbf{J} + \beta \mathbf{W}_m^T \mathbf{W}_m \quad \text{Eq. 9}$$

The matrix H to be inverted is an MxM positive definite symmetric matrix so its inverse exists. The resultant equation to be solved is:

$$(\mathbf{J}^T \mathbf{W}_d^T \mathbf{W}_d \mathbf{J} + \beta \mathbf{W}_m^T \mathbf{W}_m) \delta \mathbf{m} = \mathbf{J}^T \mathbf{W}_d^T \mathbf{W}_d (d^{obs} - \mathbf{F}[m^{(n)}]) - \beta \mathbf{W}_m^T \mathbf{W}_m (m^{(n)} - m_{ref}) \quad \text{Eq. 10}$$

This is Gauss-Newton equation.

The local quadratic representation of the true quadratic surface described by equation (Eq.5) is given by:

$$f(\delta \mathbf{m}) = \phi(m) + \mathbf{g}^T \delta \mathbf{m} + \frac{1}{2} \delta \mathbf{m}^T \mathbf{H} \delta \mathbf{m} \quad \text{Eq. 11}$$

Minimizing this with respect to $\delta \mathbf{m}$ yields the $\mathbf{H} \delta \mathbf{m} = -\mathbf{g}$. If $\mathbf{f}(\delta \mathbf{m})$ is an adequate approximation to $\Phi(\mathbf{m}^{(n)} + \delta \mathbf{m})$, then the perturbation will be good and the updated can be $\mathbf{m}^{(n+1)} = \mathbf{m}^{(n)} + \delta \mathbf{m}$. However, if $\mathbf{f}(\delta \mathbf{m})$ is a poor approximation, than the recovered $\delta \mathbf{m}$ may have a wrong direction and/or be the wrong size. There are two general strategies for dealing with such situations. The Hessian is modified and the size of a potential step is restricted so that \mathbf{f} is a good approximation. Than $\delta \mathbf{m}$ has both the correct direction and step length, and it can be added to the existing model to generate the updated solution. An other strategy is to accept that $\delta \mathbf{m}$ has the right direction but

its magnitude is incorrect. The magnitude being too large so the updated model is given by $\mathbf{m}^{(n+1)} = \mathbf{m}^{(n)} + \mu \delta \mathbf{m}$ with $0 < \mu < 1$, damping factor that reduce the step length. The combination of using the Gauss-Newton equation and step-length control produce the damped Gauss-Newton methodology.

Any of the above strategies for computing a step, can be continued until convergence has been achieved, that is until the gradient is sufficiently close to zero and the objective function don't decreases. Marquardt (1963) described an elegant method for varying smoothly between the extremes of the inverse Hessian method and steepest decent method. This method (called Marquardt method) works very well in practice and has become the standard of nonlinear least-squares problems. More implementation detail can be found in Numerical Recipes in C (Press et. al. 1992)

2.2. OPTIMIZATION METHODS

Optimization methods aim also to minimize the cost function by adjusting the model parameters but without using gradient-like techniques. Instead of that, the parameters are adjusted randomly or using systematically sampling to test the fit improvement. The three kinds of approaches presented below are the most used at this time.

2.2.1. Monte-Carlo (MC) and simulated annealing (SA) approaches

Monte-Carlo methods are pure random search methods in which model parameters m are drawn uniformly and tested against data. In such inversion process, each model parameter is allowed to vary within a predefined search interval ($m^{\min} < m < m^{\max}$), determined *a priori*. A random number rn is drawn from a uniform distribution $U[0,1]$ and then mapped into a model parameter so that:

$$m^{\text{new}} = m^{\min} + rn (m^{\max} - m^{\min}) \quad \text{Eq. 12}$$

New random models are generated by random perturbations so that calculated data can be computed for each of them. These data are compared to observed ones, so that related models can be accepted or not depending on the values of the cost function. This method implies a great number of models to be tested, for a large sampling of the parameter models to be reached (Sen and Stoffa, 1995).

In simulated annealing methods, a convergence process is searched using an iterative process in order to reduce the number of tested model parameters. Metropolis algorithm, for example, uses a Markov chain to generate new models and the decision to accept them or not are depending on a double criteria: if the cost function has been improved the new model is always accepted; if not, the model is accepted with the following probability:

$$P = \exp\left(-\frac{\Delta E}{T}\right) \quad \text{Eq. 13}$$

Where ΔE refers to the increase of the cost function between two iterations, T is a quantity called “temperature” that is adjusted to ensure the convergence (Grandjean et al., 2000).

2.2.2. Neural network

Neural networks are a particularity of SA since a large number of neurons are generated and connected, each of them corresponding to a signal pondered by a weight. These resulting signals are evaluated according to an activation function.

2.2.3. Genetic algorithms (GA)

Unlike previous approaches, which are based on analogy with a physical annealing process, genetic algorithms are based on analogy with biological evolution. These methods work with a population of model parameters coded in some suitable form. The basic steps in GA are coding, selection, crossover and mutation. Each of these steps corresponds to possible evolution from a model to another, and is therefore well established.

2.2.4. Multilevel Coordinate Search (MCS)

Inspired by a method by Jones et al. (1993), the multilevel coordinate search is a global optimization algorithm. It is guaranteed to converge if the function is continuous in the neighborhood of a global minimizer. By starting a local search from certain good points, an improved convergence result is obtained. MCS is an intermediate between stochastic (that guarantee to find a global optimum with a required accuracy) and heuristic (that find the global minimum only with high probability) optimization methods. An advantage compared to genetic algorithms, for instance, is that if the number of iterations tends to infinity, convergence can be ensured.

2.3. REVIEW OF CLASSICAL – COMMERCIAL OR NON-COMMERCIAL – CODES FOR GEOPHYSICAL DATA INVERSION

2.3.1. Geoelectric

Geoelectric data are most of the time inverted with the Res2Dinv code (Loke, 1996). The RES2DINV program uses the smoothness-constrained least-squares method inversion technique (Sasaki 1992) to produce a 2D model of the subsurface from the apparent resistivity data. It is completely automatic and the user does not even have to supply a starting model. On a Pentium based microcomputer, the inversion of a single pseudosection is usually completed within minutes. It supports the Wenner (a,b,g), Schlumberger, pole-pole, pole-dipole, inline and equatorial dipole-dipole, gradient and non-conventional arrays.

The program will automatically choose the optimum inversion parameters for a data set. However, the inversion parameters can be modified by the user. Three different

variations of the least-squares method are provided; a very fast quasi-Newton method, a slower but more accurate Gauss-Newton method, and a moderately fast and accurate hybrid technique. The smoothing filter can be adjusted to emphasize resistivity variations in the vertical or horizontal directions. It can also be optimized to produce models with smooth boundaries (for eg. chemical plumes), or with sharp boundaries (for eg. fracture zones). Resistivity information from borehole and other sources can also be included to constrain the inversion process. Three different techniques for topographic modeling (Loke 2000) are available in this program.

2.3.2. GPR

Generally, GPR signal analysis is performed using ray-tracing approximations and tomographic inversion. Several methodologies are generally adopted for determining wave propagation velocity and retrieve soil water content from GPR data (Huisman et al., 2003):

- determination of the wave propagation time to a known reflecting interface using single-offset surface GPR;
- detection of the velocity-dependent reflecting hyperbola of a buried object using single-offset surface GPR along a transect;
- extraction of stacking velocity fields from multi-offset radar soundings at a fixed central location (common midpoint method, CMP);
- determination of the ground-wave velocity for surface water content retrieval using multi- and single-offset surface GPR;
- determination of the surface reflection coefficient using single-offset off-ground GPR;
- determination of the two-dimensional (2-D) spatial distribution of water between boreholes using transmission tomography.

These basic techniques can readily be implemented and are usually available in the softwares that are provided with the commercial GPR systems. Straight-ray tomography needs more complex procedures and codes are, for instance, provided by Giroux et al. (2007) with *bh_tomo* and Sandmeier (2006) (<http://www.sandmeier-geo.de/Reflex/gpr.htm>) with *ReflexW*.

Although these approaches are well established, they still suffer from major limitations originating from the strongly simplifying assumptions on which they rely with respect to electromagnetic wave propagation phenomena. As a result, a bias is introduced in the estimates due to limited GPR model adequacy and, moreover, only a part of the information contained in the radar data is used, generally the propagation time.

Resorting to the physical basis of GPR wave propagation is necessary to estimate simultaneously both the depth dependent soil dielectric permittivity and electric conductivity. The relation between the subsurface constitutive parameters and the measured electromagnetic field is governed by Maxwell's equations. Reconstruction of the unknown constitutive parameters from the known field appeals to inverse modeling. Inverting electromagnetic data has been a major challenge in applied geophysics for many years. Successful inversion is challenging since it involves rigorous forward modeling of the 3-D GPR-subsurface system, which is furthermore computationally

very time-consuming (full-waveform inversion). Moreover, the inverse problem should satisfy elemental well-posedness conditions, which are related to the information content in the radar data. Full-waveform inversion procedures for GPR are, to the best of our knowledge, not commercially available and are subject to intensive research with 2-D (e.g., Ernst et al., 2007) and 3-D (e.g., Lambot et al., 2004; Solimene et al., 2007) codes.

2.3.3. EMI

After appropriate calibration of the instrument (for the commercial sensors), EMI directly provides, without inversion, the soil electrical conductivity that is derived from the secondary magnetic field amplitude. Yet, inversion techniques exist to reconstruct vertical electrical conductivity profiles from measurements performed at several frequencies, with different transmitter-receiver offsets, with different heights of the antennas above the ground, or with different orientations of the coils (vertical or horizontal), which result in different sensitivities with depth and thereby provide the required information (e.g., Pérez-Flores et al., 2001; Haber et al., 2004; Sasaki and Meju, 2006). Yet, they are usually applied to scales larger than the one required for near surface studies. For digital soil mapping, we have to map large areas with high resolution both laterally and in depth. These conditions imply such amount of data that make 3D or even 2D inversion too time consuming, and then 1D methods, which are extremely fast (e.g., Huang and Won, 2000; Zhang and Liu, 2001; Farquharson et al., 2003) could be more adequate to have a rapid evaluation of data. Recently, Moghadas et al. (2009) introduced a new 3D inversion procedure showing great promise for digital soil mapping using EMI, with high model adequacy and fast evaluation procedures.

2.3.4. Seismic

In the framework of the DIGISOIL project, seismic data will be processed to study surface waves dispersion (Rayleigh waves) and invert for the Shear-waves velocity variations with depth. The program used to perform such an inversion is based on Computer Programs for Seismology and is called SURF (Herrmann, 1987).

From a general point of view, these programs focus on the understanding and interpretation of seismic wave propagation in the crust and upper mantle of the Earth. Synthetic seismograph code is provided for sources and receivers at arbitrary positions in the plane layered media. Programs are provided for determination of crustal structure through the inversion of surface-wave dispersion and teleseismic P-wave receiver functions. Inversion of broadband recordings of regional earthquakes for source depth, focal mechanism and seismic moment is also provided.

In our future processing works, only the part dedicated to surface waves (surf package) will be used.

3. Adapted methodologies for DIGISOIL

3.1. ELECTRICAL METHODS

Electrical methods were initially developed in the context of mining or petroleum prospecting. We are here interested in the application of the electrical methods for the soil characterisation. In that context, electrical resistivity can be used in three ways:

- on 1D profiles (vertical soundings), to locally estimate the succession of the different horizons. By repeating these soundings in an exhaustive way, one is able to map a field site ;
- on 2D profiles, to characterise i) the evolution of the width of soil horizons on several meters or several hundreds of meters or ii) the soil bulk density or the soil structure, to see, for example, compacted clods or cracks;
- on 3D arrays, mainly to analyse the short-distance evolution of the soil structure.

Whatever the arrays (1D, 2D, 3D), the interpretation of data does not require specific tools that could not be used in other contexts than the description of soil horizons or soil structure. The constraints are not linked to the inversion tool, but to the acquisition of data: due to the very short inter-electrode spacing (from 1 m to 10 cm, sometimes even 3 cm), we have to take care of i) the distance between the electrodes, so that the interpretation of data by the model is not erroneous, ii) the hollow of the electrodes in the soil, so that the electrodes can be considered as punctual and so that the inverse model can be run properly iii) the soil surface roughness, so that the digital elevation model in the inverse model is correct ,and iv) the electrode resistance during the measurements. If all these points are taken into account, the inverse modelling can be run.

As far as 1D profiles are concerned, the interpretation of data consists in a classical sounding inversion: one considers that the earth model is a succession of horizontal layers, each layer being characterised by its width and its electrical resistivity. The inversion can usually be constrained by the knowledge of the real width of each layer, obtained in an independent way by auger holes. In the case of soil mapping, we usually use the MuCEP device, that comprises three interelectrodes spacings (Panissod et al., 1997) (see the description in Lambot et al., 2009). As a consequence, we can only interpret a very simple earth model. The inversion is done by using the QWIN1D software, that was developed at the University of Paris VI (France) and that uses the Levenberg-Marquadt optimisation algorithm (Cousin et al., 2009).

As far as 2D profiles and 3D arrays are concerned, the interpretation is done by the commercial softwares Res2DInv and Res3DInv (Loke & Barker, 1999). In common conditions, the model is used with its default parameters. It is however often

recommended to integrate the digital elevation model and to constrain the model by the width of the horizons, when they are known. To know the soil structure, there are some cases where the inverse model has to be adapted:

- in the case of albic structures, i.e. the presence of sub-vertical tongues in some degraded horizons. This type of structures is very common in lots of horizons and we can improve the use of the inverse models Res2DInv and Res3DInv by activating some options, say choosing a damping factor so that the vertical flatness filter is the double of the horizontal flatness filter

- in the case of the detection of cracks, the contrast of resistivity between the soil and the cracks are so large that the Res2DInv or Res3DInv softwares are not well adapted. A new inversion model based on the method of moments is currently being developed (Tabbagh et al., 2007) It can be now run in the direct way and permits to calculate the initial position, the width and the depth of several different cracks. It has to be improved to be run in the inverse way.

3.2. GPR – EMI

3.2.1. Electromagnetic GPR and EMI forward modeling : a united method

For both GPR and EMI, the antenna-subsurface system is modelled using a system complex, linear transfer functions, with the assumption that the distribution of the backscattered electromagnetic field measured by the antenna does not depend on the air and subsurface layers, i.e., only the amplitude and phase of the field change (local plane wave approximation over the antenna aperture). This key simplification holds when the antenna is sufficiently far above a multilayered medium, as it is the case for our off-ground, zero-offset GPR and EMI systems. The transfer function model, expressed in the frequency domain, is given by (Lambot *et al.*, 2004):

$$S_{ii}(\omega) = \frac{b(\omega)}{a(\omega)} = H_i(\omega) + \frac{H_t(\omega)G_{**}^{\uparrow}(\omega)H_r(\omega)}{1 - H_f(\omega)G_{**}^{\uparrow}(\omega)} \quad \text{Eq. 14}$$

where $S_{ii}(\omega)$ is the quantity measured by the Vector Network Analyzer (i.e., $S_{11}(\omega)$ and $S_{21}(\omega)$ for the monostatic GPR and bistatic EMI systems, respectively); $b(\omega)$ and $a(\omega)$ are, respectively, the backscattered and incident waves at the VNA reference calibration planes; $H_i(\omega)$, $H_t(\omega)$, $H_r(\omega)$ and $H_f(\omega)$ are the characteristic antenna transfer functions accounting for the antenna propagation effects and antenna-soil interactions; G_{**}^{\uparrow} is the transfer Green's function of the air-subsurface system modelled as a 3-D multilayered medium. It is worth noting that $H_t(\omega)$ and $H_f(\omega)$ play the role of global reflectances, whereas $H(\omega) = H_t(\omega)H_r(\omega)$ represents global transmitting and receiving transmittances.

The characteristic antenna transfer functions can be determined by solving a system of equations for different model configurations. To this end, we use well defined model configurations, i.e., with the antenna situated at n different heights above a perfect

electrical conductor (copper sheet), so that the Green's functions G_{**}^{\uparrow} can readily be computed and the corresponding $S_{11}(\omega)$ or $S_{21}(\omega)$ can be measured in a standard way. The system of equations (Eq.14) should be overdetermined ($n > 3$) to ensure a well-defined and accurate solution (the equations are not fully independent for the whole frequency range, depending on the measurement heights). Function $H_i(\omega)$ can also be determined in an independent way, by performing measurements in free space conditions for which $G_{**}^{\uparrow} = 0$. In that case, $H_i(\omega)$ is directly measured.

Assuming the soil surface to be located in the far field region of the antenna, the zero-offset GPR and EMI antennas reduce to a point source and receiver (point $S = (0,0,0)$ in Figure 1). For GPR, the Green's function, G_{xx}^{\uparrow} , is defined as the backscattered x -directed electric field (upward component) at the antenna phase centre for a unit x -directed electric source situated also at the antenna phase centre. Regarding EMI, for the adopted horizontal mode of operation, the source can be described as a vertical magnetic dipole and the Green's function G_{zz}^{\uparrow} is defined as the z -directed component of the backscattered magnetic field for a unit-strength z -directed magnetic source. The point source and receiver is assumed to be located above a 3-D, horizontally multilayered medium, as depicted in Figure 1. The medium consists of N layers separated by $N - 1$ planar interfaces parallel to the x - y plane of a right-handed Cartesian coordinate system. The medium of the n th layer is homogeneous and characterized by magnetic permeability μ_n , dielectric permittivity ε_n , electrical conductivity σ_n , and thickness h_n .

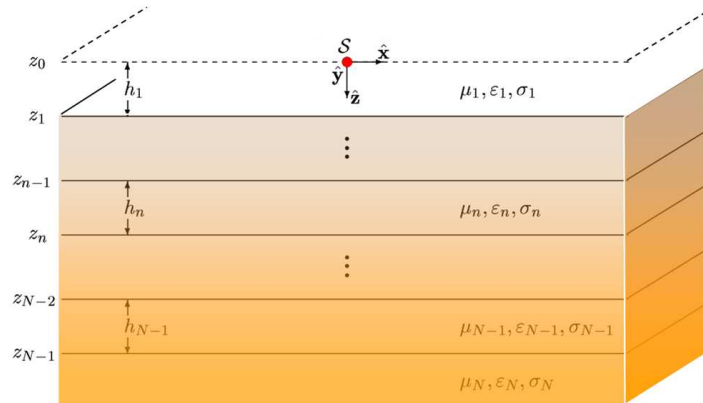


Figure 1 : Three-dimensional N -layered medium with a point source and receiver S . Each layer is characterized by the dielectric permittivity ε , electrical conductivity σ , and thickness h .

For GPR and EMI, the spatial Green's functions at the source point are respectively found to be:

$$G_{xx}^{\uparrow} = \int_0^{+\infty} \frac{1}{8\pi} \left(\frac{\Gamma_1 R_1^{TM}}{\sigma_1 + j\omega\varepsilon_1} - \frac{j\omega\mu_1 R_1^{TE}}{\Gamma_1} \right) \exp(-2\Gamma_1 h_1) k_\rho dk_\rho \quad \text{Eq. 15}$$

$$G_{zz}^{\uparrow} = \int_0^{+\infty} \left(\frac{k_{\rho}^2 R_1^{TE}}{4\pi\zeta_1\Gamma_1} \right) \exp(-2\Gamma_1 h_1) k_{\rho} dk_{\rho} \quad \text{Eq. 16}$$

where subscripts denote layer indexes, k_{ρ} is the spectral domain counterpart of the source-receiver distance, R^{TE} and R^{TM} are, respectively, the transverse magnetic (TM) and the transverse electric (TE) global reflection coefficients accounting for all reflexions and multiples from inferior interfaces, $\zeta_1 = j\omega\mu_1$, Γ is the vertical wavenumber defined as

$\Gamma = \sqrt{k_{\rho}^2 - k^2}$, whilst $k^2 = \omega^2 \mu(\epsilon - \frac{j\sigma}{\omega})$ with ω being the angular frequency. For the

free-space layer 1, we have $k_1^2 = \left(\frac{\omega}{c}\right)^2$ with c being the speed of light in free space.

The global reflection coefficients are determined recursively starting from the lower interface following the procedure presented in Slob et al. (2002). The infinite integrals (Eq.15) and (Eq.16) are evaluated by deforming the integration path in the complex k_{ρ} plane such that singularities (poles and branch points) are avoided and oscillations are minimized for proper and fast integration, respectively (Lambot et al., 2007).

Both GPR and EMI models were successfully validated in laboratory conditions. Figure 2 represents the measured and modelled GPR Green's functions for wave propagation in a two-layered sand. Figure 3 shows the measured and modelled EMI Green's functions for measurements at different heights above a copper sheet. For EMI, we observe that the model only agrees well at the loop antenna resonant frequency and when the loop is not too far from the copper sheet. As expected, elsewhere the signal-to-noise ratio is poor, resulting in larger estimation errors. In addition, when the loop antenna is relatively close to the copper sheet, the model fails to describe properly the data, as indeed the hypotheses behind the model do not hold anymore.

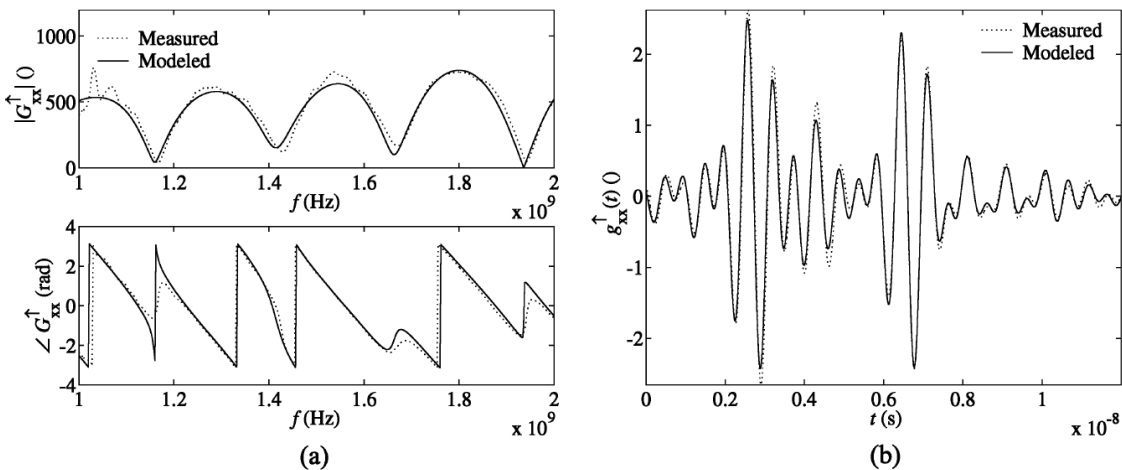


Figure 2. Measured and modelled GPR Green's functions for wave propagation in a two-layered sand. (a) Frequency domain. (b) Time domain. (Lambot et al., 2004).

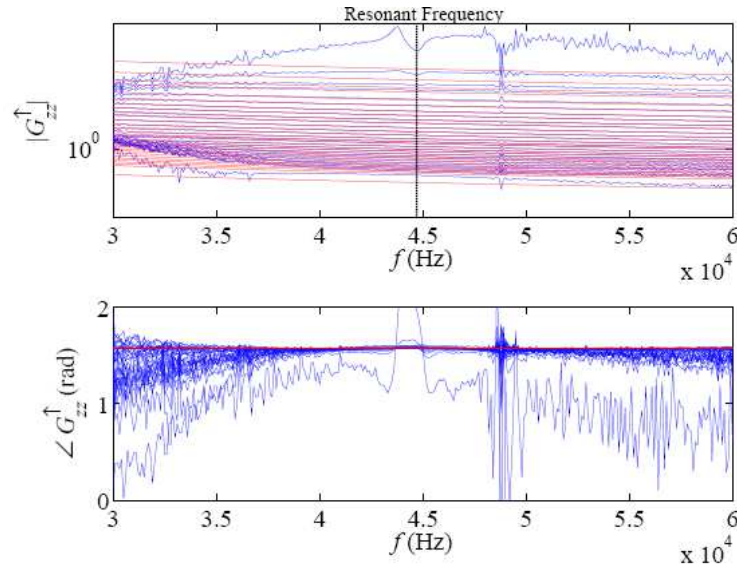


Figure 3. Measured (blue curves) and modelled (red curves) EMI Green's functions for measurements at different heights above a copper sheet. (Moghadas et al., 2009).

3.2.2. Model inversion

The soil hydrogeophysical parameters are retrieved from the GPR and EMI data by inversion of the electromagnetic model described above, resulting in a nonlinear optimization problem. In this respect, parameter vector $\mathbf{b} = [\varepsilon_n, \sigma_n, h_n]$ ($n = 1, \dots, N$) is determined from the minimization of an objective function $\phi(\mathbf{b})$. In the particular case where no prior information on the parameters is taken into account and assuming observation errors to be normally distributed, the maximum likelihood theory reduces to the classical least squares problem. The objective function expressed in terms of Green's functions (antenna effects are filtered out from the raw data) is thereby defined as follows:

$$\phi(\mathbf{b}) = (\mathbf{G}_{**}^{\uparrow*} - \mathbf{G}_{**}^{\uparrow})^T \mathbf{C}^{-1} (\mathbf{G}_{**}^{\uparrow*} - \mathbf{G}_{**}^{\uparrow}) \quad \text{Eq. 17}$$

where $\mathbf{G}_{**}^{\uparrow*} = \mathbf{G}_{**}^{\uparrow*}(\omega)$ and $\mathbf{G}_{**}^{\uparrow} = \mathbf{G}_{**}^{\uparrow}(\omega, \mathbf{b})$ are, respectively, the observed and modelled Green's functions, and \mathbf{C} is the measurement error covariance matrix. As the objective function has inherently a nonlinear topography, the minimization is carried out using the global multilevel coordinate search (GMCS) algorithm combined sequentially with the classical Nelder-Mead simplex algorithm (NMS) (Lambot et al., 2002).

Although GPR and EMI presents different sensitivities with respect to the soil electromagnetic properties and their spatial distribution (due to the different operating frequencies), both depend on the same electromagnetic quantities. It is therefore proposed to jointly invert the GPR and EMI data so that both inverse problems

regularize each other. Several data fusion techniques exist and are investigated within the DIGISOIL research activities (Lambot et al., 2009). Finally, particular inversion strategies can be designed depending on the particular application. For instance, surface or shallow soil water content can readily be obtained by performing GPR signal inversion in the time domain, by focusing on the surface reflection only (Lambot et al., 2006). In that case, the unknowns reduce to the antenna height above the soil and the soil surface dielectric permittivity. The corresponding objective function has a simple topography and can be minimized using traditional local optimization approaches, such as the Levenberg-Marquardt algorithm. Confidence intervals are also provided on the estimates to quantify uncertainty. This procedure has been used to map in real-time surface water content in the field (Figure 4).

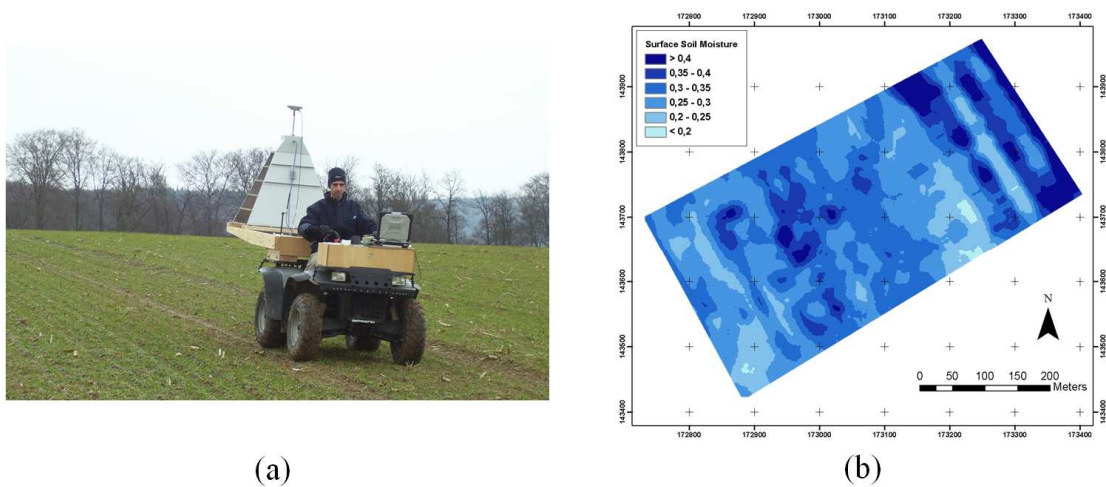


Figure 4. (a) Off-ground GPR system used for real-time mapping of the soil properties. (b) GPR-derived map of soil surface water content over a field of about 16ha, including more than 3000 measurements.

3.3. SEISMIC METHODS

The surface wave method was developed in response to needs in geotechnical engineering and S wave reflexion seismology for a non-invasive technique for estimating the in situ S wave velocity of the near surface materials.

3.3.1. Pre-processing operations

Conventional implementation of the method involves the recording of Rayleigh waves on vertical component receivers, using the Rayleigh wave data to estimate the phase velocity dispersion curve, and then applying the method of geophysical inversion to the dispersion curve to obtain the S wave velocity as a function of depth.

It is very important to recognize that the above steps are unconnected and their interaction must be adequately accounted for during the whole interpretation process.

Several approaches can be used to process field data in order to get the experimental dispersion curve. The phase velocity can be evaluated on the basis of the phase difference between a couple of receivers or from the simultaneous processing of several trace. Here we use, a transform based method, based on transformation of experimental data from time offset domain to intercept time ray parameter (McMechan and Yeldin 1981; Moktar *et al.* 1988):

$$U(v, f) = \sum_{i=1}^N C^{-1}(f) A(x_i, f) e^{j\varphi_i} e^{-\frac{2\pi j f x_i}{v}} \quad \text{Eq. 18}$$

where $\mathbf{A}(x_i, f)$ is the amplitude spectrum of the trace i at distance x_i , N is the number of traces in the shot gather, and $C(f)$ is the amplitude spectrum of the first trace. The dispersion curve is directly obtained by picking the maximal values of the modulus of $U(v, f)$. This curve is used to determine the shear wave velocity via inversion process.

3.3.2. Strategy for inversion

A stack of L horizontal layer over a half space is the most common discrete parameterization for inversion of surface wave dispersion curve. Each layer is assumed to be homogeneous and isotropic linearly elastic medium. The parameters for layer j are typically chosen to be the thickness h_j , \mathbf{S} wave velocity $\mathbf{V}s_j$, \mathbf{P} wave velocity $\mathbf{V}p_j$ and density ρ_j . A parameter vector \mathbf{p} with $\mathbf{M}=4(\mathbf{L}+1)$ parameters is used to represent the complete set of all parameters (Figure 5).

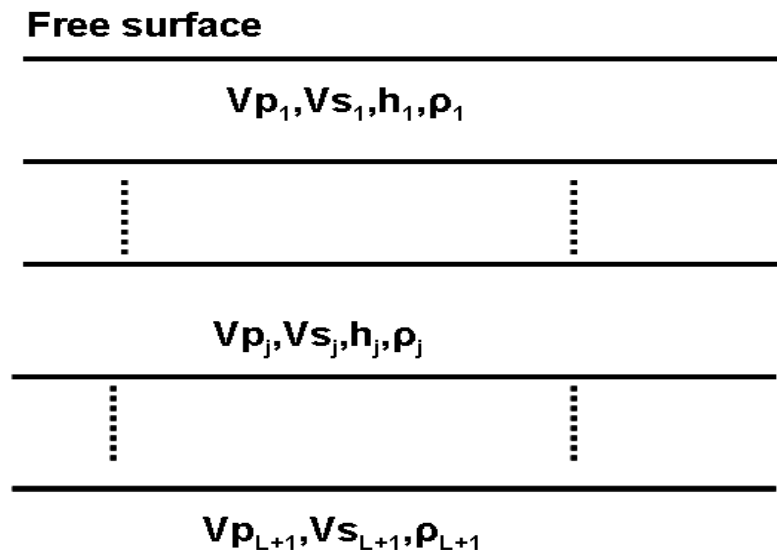


Figure 5 : Subsurface model commonly used for surface wave inversion

The observed data consist of $\mathbf{N} > \mathbf{M}$ phase velocities $\mathbf{c}(f_i)$ at a given set of frequencies f_i

$$c = [c(f_1), c(f_2), c(f_3), \dots, c(f_n)] \quad \text{Eq. 19}$$

The data are to be compared with **N** theoretical phase velocities $c_t(f_i)$ computed for the same mode, and the frequencies f_i .

$$c_t = [c(f_1, p), c(f_2, p), c(f_3, p), \dots, c(f_n, p)] \quad \text{Eq. 20}$$

where trial values are used for the elements of the parameter vector **p**.

Here, the forward problem is the computation of theoretical phase velocities for layered elastic subsurface. It is typically a process of finding the roots of a dispersion equation which represents the constraints imposed on surface wave propagation in the layered model. Numerous specific methods exist for computing theoretical dispersion curve for a layered medium. We use the Thomson-Haskell matrix method that is a special case of the more general formulation of elastic wave propagation in a vertically heterogeneous medium (Herrmann, 1987).

Given a discrete parameterisation and the solution to the forward problem, the inversion is carried out by searching parameter space for one parameter vector **p_a** that minimises an objective function. The most basic objective function **Φ(p)** is the cumulative squared discrepancy between the observed and theoretical data

$$\phi(p) = [c - c_t][c - c_t]^T \quad \text{Eq. 21}$$

where T indicates the transpose. The search for **p_a** may proceed iteratively through a limited portion of parameter space from an initial guess **p₀**, or it may be a global search which is conducted over the entire parameter space.

Regardless of the search strategy, inversion of surface wave data suffers from non uniqueness. More than one parameter vector can be regarded as acceptably minimizing the objective function. Non uniqueness may be addressed by adding a priori information and by adding a reasonable global constraint to the range of S wave velocities. It is common to fix the values of P wave velocity and density during inversion because the inversion is relatively less sensitive to these parameters (Bitri et al., 1998, Xia et al. 1999).

The inversion of surface wave for near surface properties has undergone significant development in recent years that has greatly enhanced its capabilities (Xia et. al., 1999, Lai et al. 2005, Del Moro and Pipan, 2007).

The recent developments carried out in BRGM allow this technique to be carried out along linear structures and for mapping natural hazards such as basement topography, soil stiffness, etc. Important efforts were deployed, particularly for the source signal generation and for the sensor line manipulation. To increase the speed and efficiency of surface wave data recording and thereby keep acquisition costs down, a new type of multichannel seismic cable has been designed and manufactured. It consists of 24 takeouts at fixed 0.5m intervals. Each takeout is attached to a single 10Hz vertical geophone. The seismic cable is towed behind a vehicle. A 24-channel Geometrics

Geode seismograph was used to record impact from a 1-kg hammer. Each 24-trace shot gather was analysed with SIRayD (Grandjean and Bitri, 2006), facilitating the use of surface wave with continuous profiling techniques. For each shot, dispersion curve was individually inverted into a depth versus shear-wave velocity profile. The linearized iterative least-squares technique used here is adapted from Herrman (1987). A 2D contour plot of the shear-wave velocity field was produced by gathering all the velocity profiles into sequential order, according to half shot station.

3.3.3. Proposed solution: methodology and code

The SASW method allows to obtain a velocity model at a given point because of the dispersive character of surface waves. The dispersion diagram reveals the dependence of phase velocity with frequency. To obtain the dispersion diagram, data are first recorded by seismic receivers ((x, t) domain) and transformed in the (x, ω) domain by a fast Fourier transform (FFT). A second transformation is performed to represent data in the (p, ω) domain where p is the ray parameter (McMechan and Yedlin, 1981; Mokhtar et al, 1988). The spectrum of the trace i is:

$$A(x_n, \omega) e^{j\phi_i(\omega)} \quad \text{Eq. 22}$$

The energy stack for N traces so corresponds to :

$$U(p, \omega) = \sum_{n=1}^N C^{-1}(\omega) A(x_n, \omega) e^{j\phi_i} e^{j\omega p x_n} \quad \text{Eq. 23}$$

Where p is fixed and C(ω) is the spectrum of the first trace.

The maximum of the obtained energy ($|U(p, \omega)| \max$) for each value of the ray parameter is associated to a frequency and then, the dispersion curve is obtained. More than one propagation mode (m) can constitute the dispersion diagram.

After this stage, the inversion process of dispersion curves aims to find the vertical S-waves velocity model. The observed real dispersion curve, compared to synthetic curves computed from an *a priori* velocity model, generate phase velocity residues. The initial model is described by 4 parameters: layer thickness, density and P/S waves velocity. The model of S-waves velocity and layers thicknesses can be obtained by inversion of dispersion curves which mainly depends on these 2 parameters. Consequently, it is not necessary to estimate the P-waves velocity model and density of layers with accuracy. In our processing sequence, parameters of the initial model are thus calculated using the phase velocity values. For an elastic media with Poisson coefficient of 0.38, following relations are used:

$$V_s = V_p * 1.1$$

$$V_p = 2.4 * V_s$$

$$\text{Rho} = 2.5 - 0.0002 * (4000 - V_p)$$

Concerning the penetration depth of surface waves, the following empirical relation found in literature is used:

$$Z = 0.53 V_{ph}/f \quad \text{Eq. 24}$$

Where f is the frequency of surface waves.

A linearized inversion method is used then to obtain the S-waves velocity model and layers thicknesses (Figure 6). For each iteration in the inversion process, the algorithm tends to fit a computed dispersion curve to observed real data.

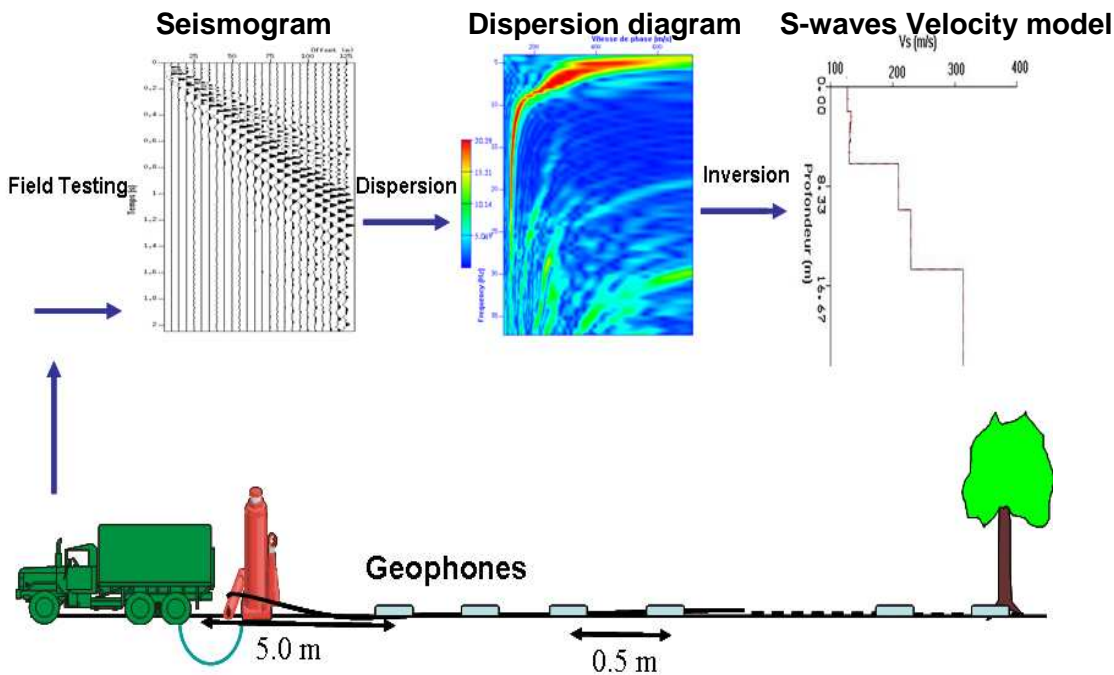


Figure 6 : From acquisition to inversion of surface wave.

To facilitate and make shorter the time required for processing of all seismic measurements, an automatic picking code is proposed (Figure 7). The algorithm finds the maximum of the dispersion diagram for each frequency in the chosen domain to define a global shape of the dispersion curve. Those are collected in a M by N matrix where M defines the number of samples from the frequency discretisation and N the number of seismic shots and represented as a surface. Such representation allows the analysis of lateral variability of surface waves dispersion along seismic sections. Different tools of image processing and/or polynomial interpolation are available for adjusting curves to the inversion input criteria.

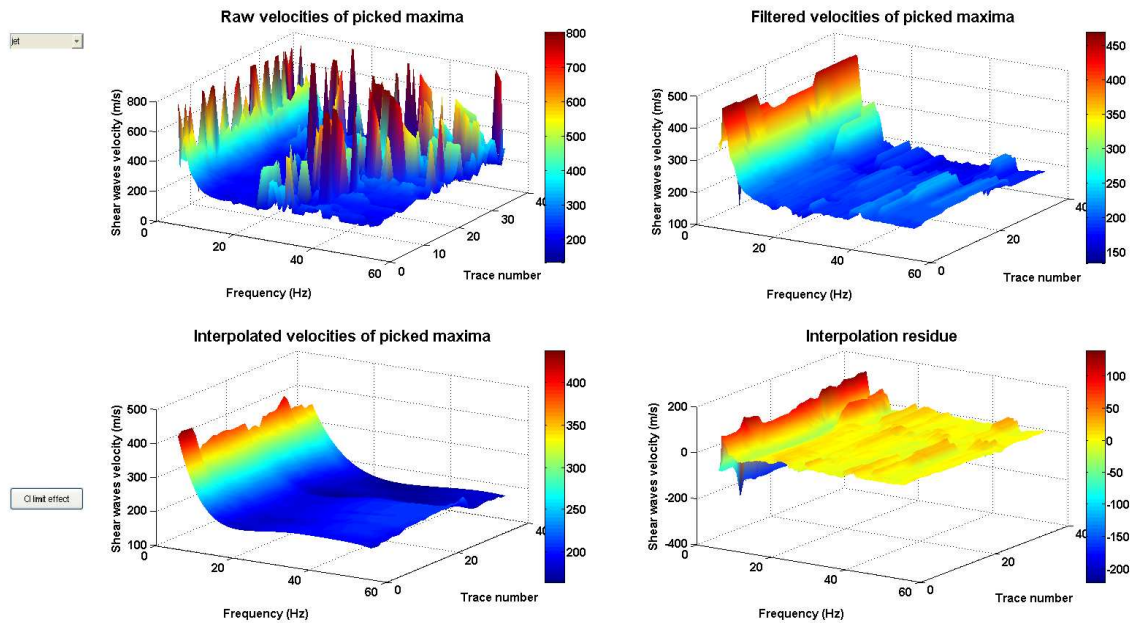


Figure 7 : Automatic extraction of dispersion curves and shape processing.

The output of the proposed solution for seismic data processing is a vertical S-waves velocity model at one point. For DSM, measurements are performed along a regular grid defined over the studied zone (Figure 8). Soil properties (density, thickness, velocity etc.) deduced from geophysical parameters (V_s), defined at each point of the grid, are then interpolated by kriging technique to generate a map and deliver a spatial investigation of the properties variability.

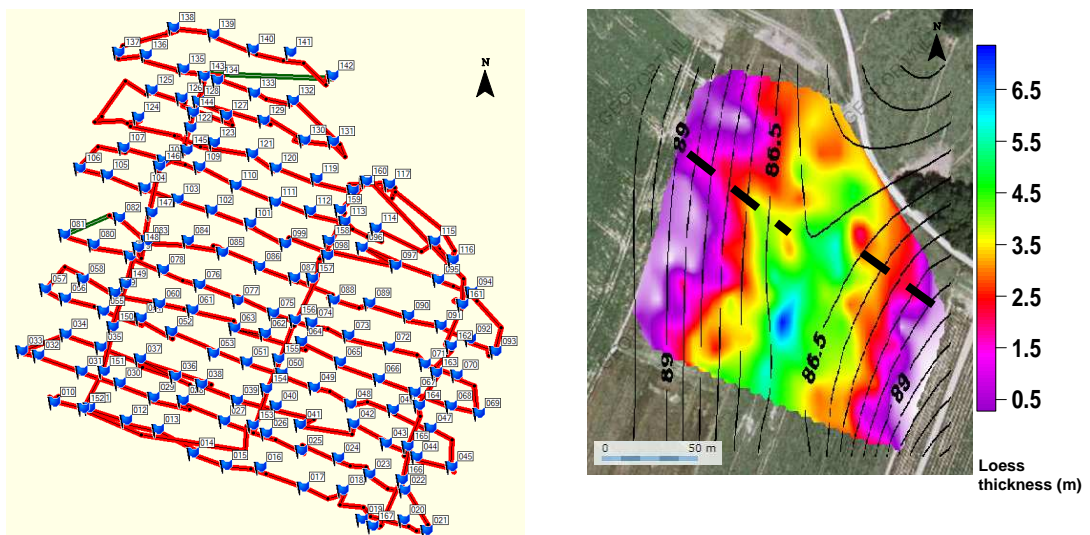


Figure 8 : Spatial covering of a studied area (left) and associated soil property map (right).

4. Conclusions

This deliverable presents some elements for retrieving geophysical parameters from sensors measurements. In order to reach the physical frontiers of information retrieval from the different sensors, signal processing, when possible, is described. It is mainly based on advanced mechanistic inverse modelling techniques. Efforts are focus on the presentation of improved signal understanding, forward modelling, and inversion using global optimization and regularization to estimate the soil geophysical parameters.

A preliminary section is dedicated to give an overview of the fundamentals of inversion / optimization processes used in geophysics. In a second part, specificities of algorithms developed or adapted in the framework of the DIGISOIL project are described particularly for GPR, EMI, Geoelectric and seismic methods. Some examples of application are also shown.

5. References

- Bitri A., Le Begat S. and Baltassat J.M. 1998. Shear wave velocity determination of soils from in-situ Rayleigh wave measurements. Proceedings of 4th EEGS Meeting, Barcelona, Spain, pp. 503–506.
- Cousin I., Besson A., Bourennane H., Pasquier C., Nicoulaud B., King D., Richard G., 2009. From spatial-continuous electrical resistivity measurements to the soil hydric functioning at the field scale. *Comptes Rendus Géosciences* (accepted)
- Del Moro, G., and Pipan, M., 2007. Joint inversion of surface wave dispersion curves and reflexion travel time via multi-objective evolutionary algorithms. *Journal of applied geophysics*. 61 (1) 56-81.
- Ernst, J.R., Maurer, H., Green, A.G. and Holliger, K., 2007. Full-waveform inversion of crosshole radar data based on 2-D finite-difference time-domain solutions of Maxwell's equations. *IEEE Transactions on Geoscience and Remote Sensing*, 45(9): 2807-2828.
- Farquharson, C.G., Oldenburgh, D.W., Routh, P.S., 2003. Simultaneous 1D inversion of loop-loop electromagnetic data for magnetic susceptibility and electrical conductivity. *Geophysics* 68 (6), 1857–1869.
- Lai, C.G., Rix, G.J., Foti, S., 2005. Propagation of data uncertainty in surface wave inversion. *Journal of Environmental and Engineering Geophysics*.10 (2) 219-228.
- Giroux, B., Gloaguen, E. and Chouteau, M., 2007. bhtomo - a Matlab borehole georadar 2D tomography package. *Computers and Geosciences*, 33(1): 126-137.
- Grandjean G. and Bitri A., 2006. 2M-SASW: inversion of local Rayleigh wave dispersion in laterally heterogeneous subsurfaces: application to Super-Sauze landslide (France). *Near Surface Geophysics*,, 367-375.
- Grandjean G., Bitri A. & Guillen A., 2000. Least squared generalized inversion coupled with Metropolis optimization for estimating shear wave velocities from Rayleigh wave measurements. EEGS, Bochum, Germany.
- Haber, E., Ascher, U.M., Oldenburg, D.W., 2004. Inversion of 3D electromagnetic data in frequency and time domain using an inexact all-at-once approach. *Geophysics* 69 (5), 1216–1228.
- Hermann, R.B., 1987. Computer programs in seismology. Saint-Luis University, USA.
- Huang, H., Won, I., 2000. Conductivity and susceptibility mapping using broadband electromagnetic sensors. *Journal of Environmental and Engineering Geophysics* 5 (4), 31–41.
- Huisman, J.A., Hubbard, S.S., Redman, J.D. and Annan, A.P., 2003. Measuring soil water content with ground penetrating radar: A review. *Vadose Zone Journal*, 2: 476-491.

- Jones, D. R., Perttunen, C. D. and Stuckman, B. E. (1993), Lipschitzian Optimization without the Lipschitz Constant, *J. of Optimization Theory and Applications* 79, 157–181.
- Lai, C.G., Rix, G.J., Foti, S., 2005. Propagation of data uncertainty in surface wave inversion. *Journal of Environmental and Engineering Geophysics*.10 (2) 219-228.
- Lambot, S., Javaux, M., Hupet, F. and Vanclooster, M., 2002. A global multilevel coordinate search procedure for estimating the unsaturated soil hydraulic properties. *Water Resources Research*, 38(11): 1224, doi:10.1029/2001WR001224.
- Lambot, S., Slob, E.C., van den Bosch, I., Stockbroeckx, B. and Vanclooster, M., 2004. Modeling of ground-penetrating radar for accurate characterization of subsurface electric properties. *IEEE Transactions on Geoscience and Remote Sensing*, 42: 2555-2568.
- Lambot, S., E.C. Slob, M. Vanclooster, and H. Vereecken. 2006. Closed loop GPR data inversion for soil hydraulic and electric property determination. *Geophysical Research Letters* 33:L21405, doi:10.1029/2006GL027906.
- Lambot, S., Slob, E. and Vereecken, H., 2007. Fast evaluation of zero-offset Green's function for layered media with application to ground-penetrating radar. *Geophysical Research Letters*, 34: L21405, doi:10.1029/2007GL031459.
- Lambot S., Grandjean G., Samyn K., Cousin I., Thiesson J., Stevens A., Chiarantini L, 2009. Technical specifications of the system of geophysical sensors. Report N° FP7-DIGISOIL-D1.1, 86 p.
- Lambot, S., F. André, D. Moghadas, E.C. Slob, and H. Vereecken, Analysis of full-waveform information content in ground penetrating radar and electromagnetic induction data for reconstructing multilayered media, *Proceedings of the 2009 5th International Workshop on Advanced Ground Penetrating Radar*, 5 pages, IWAGPR 2009, Grenada, Spain, 27-29 May 2009 (in press).
- Loke, M.H., 2000. Topographic modelling in resistivity imaging inversion. 62nd EAGE Conference & Technical Exhibition Extended Abstracts, D-2.
- Loke M.H., R.D. Barker, 1996. Rapid least square inversion of apparent resistivity pseudosections using a quasi-Newton method, *Geophysical Prospecting* 44 131-152.
- Moghadas, D., André, F., Vereecken, H. and Lambot, S., 2009. Efficient loop antenna modeling for zero-offset, off-ground electromagnetic induction in multilayered media. *IEEE Transactions on Geoscience and Remote Sensing*, Submitted.
- Oldenbourg., W., D. and Li., Y. 2005. Inversion for applied geophysics: A tutorial. In *Near Surface Geophysics. Investigation in geophysics No 13*.
- Panissod, M. Dabas, A. Jolivet & A. Tabbagh, 1997. A novel mobile multipole system (MUCEP) for shallow (0-3m) geoelectrical investigation: the 'Vol-de-canards' array, *Geophysical Prospecting* 45 983-1002.
- Pérez-Flores, M.A., Méndez-Delgado, S., Gómez-Treviño, E., 2001. Imaging low frequency and dc electromagnetic fields using a simple linear approximation. *Geophysics* 66 (4), 1067–1081.

- Sasaki, Y. 1992. Resolution of resistivity tomography inferred from numerical simulation. *Geophysical Prospecting*, 40, 453-464.
- Sasaki, Y., Meju, M.A., 2006. A multidimensional horizontal-loop controlled source electromagnetic inversion method and its use to characterize heterogeneity in aquiferous fractured crystalline rocks. *Geophysical Journal International* 166, 59–66.
- Sen, M. and Stoffa, P.L., 1995. Global optimization methods in geophysical inversion., In: *advances in exploration geophysics*, 4, Elsevier, 281p.
- Scales, J and Smith, M., 1996. *Introductory geophysical inverse theory*: Samizdat Press.
- Samyn, K., O. Cerdan, G. Grandjean, A. Bitri, S. Bernardie, J.F. Ouvry, Soil depth mapping using seismic surface waves for the assessment of soil vulnerability to erosion. EGU 2009, Vienna, Austria.
- Slob, E.C. and Fokkema, J., 2002. Coupling effects of two electric dipoles on an interface. *Radio Science*, 37(5): 1073, doi:10.1029/2001RS2529.
- Solimene, R., Soldovieri, F., Prisco, G. and Pierri, R., 2007. Three-dimensional microwave tomography by a 2-D slice-based reconstruction algorithm. *IEEE Geoscience and Remote Sensing Letters*, 4(4): 556-560.
- Tabbagh J., Samouëlian A., Cousin I., Tabbagh A., 2007. Numerical modelling of direct current electrical resistivity for the characterisation of cracks in soils. *Journal of Applied Geophysics*, 62, 4, 313-323. Doi: 10.1016/j.jappgeo.2007.01.004
- Tarantola, A., 1987, *Inverse problem theory*. Elsevier Science Publishing Co., Inc.
- McMechan G.A. and Yedlin M.J. 1981 Analysis of dispersive waves by wave field transformation. *Geophysics* 46, 869–874. Menke, W., 1989. *Geophysical data analysis: Discrete inverse theory*: Academic Press.
- Mokhtar, T. A., Herrmann, R. B., and Russel, D. R. 1988 Seismic velocity and Q model for the shallow structure of the Arabian shield from shot-period Rayleigh waves, *Geophysics*, 53, 1379-1387.
- Press. W., Teukolsky S.A., Vetterling. W.T., and Flanery B.P., 1992. *Numerical recipes in C. The art of scientific computing*. Cambridge University Press.
- Xia J., Miller R.D. and Park C.B. 1999. Estimation of near-surface shear wave velocity by inversion of Rayleigh wave. *Geophysics* 64, 691–700.
- Zhang, Z., Liu, Q., 2001. Two nonlinear inverse methods for electromagnetic induction measurements. *IEEE Geoscience and Remote Sensing* 39 (6), 1331–1339.



Scientific and Technical Centre
ARN Division
3, avenue Claude-Guillemain - BP 36009
45060 Orléans Cedex 2 – France – Tel.: +33 (0)2 38 64 34 34